

2012-2

Evaluation and Identification of Markers of damage in Mushrooms (*Agaricus Bisporous*) Postharvest Using a GC/MS Metabolic profiling Approach.

Aoife O'Gorman

Technological University Dublin, aoife.ogorman@tudublin.ie

Catherine Barry-Ryan

Technological University Dublin, Catherine.Barryryan@tudublin.ie

Jesus Maria Frias

Technological University Dublin, Jesus.Frias@tudublin.ie

Follow this and additional works at: <https://arrow.tudublin.ie/schfsehart>

 Part of the [Food Chemistry Commons](#)

Recommended Citation

O'Gorman, A., Barry-Ryan, C. and Frias, J. M. Evaluation and Identification of Markers of damage in Mushrooms (*Agaricus Bisporous*) Postharvest Using a GC/MS Metabolic profiling Approach. *Metabolomics*, February 2012, Volume 8, Issue 1, pp 120-132. doi:10.1007/s11306-011-0294-3

This Article is brought to you for free and open access by the School of Food Science and Environmental Health at ARROW@TU Dublin. It has been accepted for inclusion in Articles by an authorized administrator of ARROW@TU Dublin. For more information, please contact arrow.admin@tudublin.ie, aisling.coyne@tudublin.ie.



This work is licensed under a [Creative Commons Attribution-Noncommercial-Share Alike 4.0 License](#)

Evaluation and identification of markers of damage in mushrooms (*Agaricus bisporus*) postharvest using a GC/MS metabolic profiling approach

Aoife O’Gorman, Catherine Barry-Ryan and Jesus M. Frias*

School of Food Science & Environmental Health, Dublin Institute of Technology,
Cathal Brugha Street, Dublin 1, Ireland.

* Corresponding author. Tel +353 1 402 2259, Fax +353 1 402 4495

E-mail: jesus.frias@dit.ie

We acknowledge financial support from the Irish Department of Agriculture and Food under the Food Institutional Research Measure (FIRM), supported through EU and national funds.

Abstract

The aim of this research was to use the gas mass spectrometry (GC/MS) profiling method coupled with chemometric tools to profile mechanically damaged and undamaged mushrooms during storage and to identify specific metabolites that may be used as markers of damage. Mushrooms grown under controlled conditions were bruise damaged by vibration to simulate damage during normal transportation. Three damage levels were evaluated; undamaged, damaged for 20 min and damaged for 40 min and two time levels studied; day zero and day one after storage at 48C. Applying this technique over 100 metabolites were identified, quantified and compiled in a library. Random forest classification models were used to predict damage in mushrooms producing models with error rates of 10% using cap and stipe tissue. Fatty acids were found to be the most important group of metabolites for predicting damage in mushrooms. PLS models were also developed producing models with low error rates.

With a view to exploring biosynthetic links between metabolites, a pairwise correlation analysis was performed for all polar and non-polar metabolites. The appearance of high correlation between linoleic acid and pentadecanoic acid in the non-polar phase of damaged mushrooms indicated the switching on of a metabolic pathway when a mushroom is damaged.

Keywords

GC/MS; Metabolic profiling; Mushrooms; Damage; Chemometrics

1. Introduction

Gas chromatography coupled to mass spectrometry (GC/MS) is one of the most frequently used tools for profiling primary metabolites (Fiehn, 2008). Over the past number of years metabolomics has emerged as a field of increasing interest to food scientists (Gibney *et al.*, 2005; García-Cañas *et al.*, 2010), with applications ranging from profiling of plant species (Arbona *et al.*, 2009), to discriminating between food spoilage bacteria (Needham *et al.*, 2005), to studying the effects of stress and so forth (Roessner-Tunali *et al.*, 2003). As a metabolite profiling technique, GC/MS has been used to detect and discriminate fungal diseases in mango (Moalemiyan *et al.*, 2007), and to study potatoes (Roessner *et al.*, 2000; Dobson *et al.*, 2008), pears (Pedreschi *et al.*, 2009), tomatoes (Schauer *et al.*, 2005) and apples (Vikram *et al.*, 2004).

The white mushroom (*Agaricus bisporus*) is one of the most widely cultivated and consumed of all edible fungi worldwide and the market for this product continues to develop because of interest in its dietary and health benefits (Chang and Miles, 2004). *Agaricus bisporus* is one of the most important horticultural crops grown in Ireland with more than 60000 tons produced annually (Teagasc, 2007). Mushrooms are delicate foodstuffs that are very sensitive to inappropriate handling and transportation practices, which can result in injuries on the mushroom causing cap discoloration. The major cause of quality loss that accounts for the reduction in market value of mushrooms is postharvest browning (Jolivet *et al.*, 1998; Burton, 2004). Mechanical damage triggers the browning process within mushroom tissues changing the metabolic state of the mushroom.

Recent studies have demonstrated a number of spectroscopic and imaging techniques as being important tools for the investigation of various mushroom quality-related issues, such as mechanical damage (Esquerre *et al.*, 2009) and freeze damage

detection (Gowen *et al.*, 2009); however, there is a need to investigate specific metabolites and metabolic pathways that may be related to browning in order to understand it fully.

The objective of this study was to use GC/MS to profile damaged and undamaged mushrooms, building a library of mushroom specific metabolites. The GC/MS data would then be coupled with chemometric methods to develop models to (a) predict damage in mushrooms and (b) attempt to identify specific metabolites as makers of damage. The analysis of the metabolic profile of mushrooms will enable metabolic targets to be found that are related to mechanical damage and also help to identify new genetic traits that may be used for varietal improvement. A secondary aim was to use the data to explore mushroom biochemistry, with a view to detecting any unexpected close linkages between metabolites, by applying correlation analysis.

2. Material and Methods

2.1. Experimental Design

Second flush mushrooms were grown at the Teagasc Research Centre Kinsealy (Dublin, Ireland), harvested damage-free. A set of 120 closed cap, defect free *Agaricus bisporus* strain Sylvan A15 (Sylvan Spawn Ltd., Peterborough, United Kingdom) mushrooms (3-5 cm cap diameter) were selected for this study and immediately transported by road to the testing laboratory. Special trays were designed to hold mushrooms by the stem using a metal grid to avoid contact between (a) mushrooms and (b) between the top of mushroom caps and the tray lid during transportation. A subset of 80 mushrooms was subjected to physical damage using a mechanical shaker (Gyrotory G2, New Brunswick Scientific Co., USA) set at 300 rpm; two damage levels were chosen damaged for 20 minutes (D20) and damaged for

40 minutes (D40), which correspond to threshold quality and unacceptable L-values for mushrooms respectively (Gormley and O'Sullivan, 1975). The remaining 40 mushrooms were untreated and labeled as undamaged (UD). Samples were analyzed on day zero and day one after storage at 4°C. Twenty mushrooms were selected for each day and damage level. Sample preparation involved the manual dissection of each mushroom into its three main tissue types (cap, gills and stipes) before freezing overnight at -70°C in a cryogenic fridge (Polar 340V Cryogenic fridge, Angeelantoni Industrie spA, Massa Martana, Italy) until further processing. Extraction, fractionation and methoxyamination of carbonyl moieties, followed by derivatisation of acidic protons with N-methyl-N-(trimethylsilyl)-trifluoroacetamide (MSTFA) prior to GC/MS analysis was performed as described previously (Lisec *et al.*, 2006) with minor modifications.

2.2. Extraction of Polar & Non-polar Metabolites from Freeze-Dried Powder

Two hundred mg of frozen mushroom tissue and 1 ml of methanol (Sigma Aldrich, Dublin, Ireland) were added to an eppendorf tube and homogenised using a vortex mixer for 10 sec. Two internal standard (IS) compounds were added to the eppendorf tube, one polar (ribitol) and one non-polar (nonadecanoic acid). The IS solutions were 0.5 µl of 0.2 mg / ml of distilled water solution of ribitol (Sigma Aldrich, Dublin, Ireland) and 50 µl of 0.2 mg / ml of CHCl₃ solution of nonadecanoic acid (Sigma Aldrich, Dublin, Ireland). The contents of the eppendorf were then mixed with a vortex mixer for 10 sec. Samples were then placed in a heating bath for 15 min at 70°C. The different phases were then separated using a Micro Centrifuge 4212 (Medical Supply Co. Ltd., Dublin, Ireland) at 14000 rpm for 5 min. The supernatant

(polar phase) was transferred from the eppendorf using a 200 μ l micropipette and placed in a Teflon tube and mixed with 1 ml of distilled water.

An aliquot of 750 μ l of chloroform was added to the pellet (non-polar phase) and shaken in a water bath for 5 min at 37°C. Following centrifugation at 14000 rpm for 5 min the supernatant of the non-polar phase was transferred to the same Teflon tube as the polar phase and homogenized with the methanol, distilled water and chloroform using the vortex. The remaining phase was discarded.

The polar phase was separated from the lipid phase into a new eppendorf tube and dried in a freeze-dryer (Micro-modulyo, EC Apparatus, New York, USA) for 24 hours.

2.3. Transmethylation & Derivatization of Non-polar Phase

To extract the non-polar phase 900 μ l of CHCl_3 and 1 ml of MeOH solution containing 3 % v/v H_2SO_4 (Sigma Aldrich, Dublin, Ireland) were added to the Teflon tubes. The lipids and free fatty acids were transmethylated for 4 h in an oil bath at 100°C. The next step involved removing any remaining polar phase; 4 ml of distilled water was added to the Teflon tube. After homogenisation using a vortex mixer and centrifugation at 4000 rpm for 15 min, the water phase was removed. This procedure was conducted twice. The lipid phase was transferred to a glass vial which was left unscrewed for 24 h or more to allow the chloroform to evaporate. After evaporation, 10 μ l of pyridine solution (20 mg of methoxyamine hydrochloride / ml pyridine) and 10 μ l of the silylation agent N-methyl-N-trimethylsilylfluoracetamide (MSTFA, Sigma Aldrich, Dublin, Ireland) were added to the vials. After silylation for 30 min at 37°C, 1 μ l was injected into the GC/MS. A total of 360 non-polar injections were taken.

2.4. Derivatization of Polar Phase

When the polar phase was dried, 50 μ l of methoxyamine hydrochloride (20 mg/ml pyridine) was added and the solution was mixed using a vortex mixer. The sample was placed for 90 min in a shaking water bath at 37°C for 30 min. The sample was then stored at room temperature for 120 min and 1 μ l was injected into the GC/MS. A total of 360 injections were taken.

2.5. GC/MS Analysis

The polar and non-polar samples were analyzed similarly using a GC/MS system comprised of a Varian CP-3800 gas chromatograph with CP-8410 autosampler coupled to a Varian Saturn 2200 quadrupole MS running in EI+ mode (JVA Analytical Ltd., Dublin, Ireland). Chromatography was performed on a Cp-sil 24 CB low bleed/MS capillary column (length 30 m, diameter 0.25 mm and film thickness 0.25 μ l) using helium at 1.0 ml/min. Data were acquired using the Saturn software (Saturn GC/MS WS Ver 5.5, Varian Inc, USA).

2.6. Data Analysis

A number of raw GC/MS data files were selected as representative examples for both polar and non-polar metabolites. These files were used with the Automated Mass Spectral Deconvolution and Identification System (AMDIS, V2.1, NIST, USA) software package to verify the presence of individual analytes and to deconvolute co-eluting peaks. Specific ion characteristics of each metabolite were selected to be used for chromatogram detection in processing methods. Compounds were identified by analysis of standards, comparison with libraries and literature data. During the analysis of the chromatograms the following steps were taken:

- The chromatogram components were deconvoluted and the baseline noise subtracted with representative MS spectra selected.
- In a preliminary search with a reduced number of sample chromatograms, the representative spectrum of every component was compared with the NIST library of MS spectra (NIST Mass Spectral Search Programme Version 1.7a, USA, 2001).
- Compounds identified which yielded weighted probabilities of over 70% were compiled in a library for automated batch search, which is an acceptable level to avoid false positives as reported by Norli and colleagues (Norli *et al.*, 2010).
- An automated analysis to report the presence and quantification of all the compounds in the library was performed by analysis of MS spectra and retention index. The quantification of the compound concentration was done through the use of internal standard area and the known concentration of the internal standard.
- A matrix table with the concentration of each selected library metabolite in each of the samples was produced in the batch job, complete with sample information (i.e. phase, tissue, storage age and damage level) and used for multivariate analysis.

2.7. Chemometric Data Analysis

Processed data were subjected to multivariate and statistical analyses using the statistical package R (Version 2.10.0) (R_Development_Core_Team, 2009). The analysis of GC/MS data involved the following steps:

1. A preliminary observation of the data using principal component analysis (PCA) to identify clusters of data and outliers as appropriate.
2. Modeling the data using random forests (RF) (Breiman, 2001) was performed in order to (a) discriminate between damaged and undamaged mushrooms and (b) to identify specific metabolites as markers of damage in mushrooms. The number of trees fitted to build the random forest was 1000, the number of random metabolites was set at 100 after optimization and the RF model trained was made using a stratified random sampling strategy of the targeted/identified metabolites that would take the same number of metabolites from each of the tissues.
3. Univariate statistics (ANOVA) were used to assess the ability of the identified metabolites (as identified by the RF models) which may be used for the identification of markers of damage.
4. Partial least squares discriminant analysis (PLS-DA) using the indications of the PCA and optimizing the hyperparameter of the number of components in the PLS regression step was performed. Confusion matrices for the training and test sets were used to identify the ability of PLS-DA models to discriminate damage. PLS-DA analysis was performed using the Caret (classification and regression training) package in R (R_Development_Core_Team, 2009).
5. Correlation analyses were performed on the polar and non-polar metabolites separately for each damage level and mushroom age. Pair-wise correlation was performed on the response ratios of all metabolites. Two metabolites were considered to be highly correlated if the coefficient had a value of ≥ 0.9 . Medium correlated metabolites had coefficient value of $\geq 0.7-0.9$. This

approach can identify both biosynthetically related and co-ordinately regulated metabolites (Steuer *et al.*, 2003; Dobson *et al.*, 2008).

3. Results and Discussion

3.1. Metabolites

During the analysis of the 720 chromatograms a library with 105 metabolites was built. Table 1 contains 62 metabolites from both polar and non-polar chromatograms, a number (44) of metabolites were not included in the table as they were only found in a very small percentage of chromatograms (<10%). In the non-polar chromatograms a number of fatty acids and phenolic compounds were identified. Sugars, polyols and amino acids were identified in polar phase chromatograms. Since authentic chemical standards were not run for every metabolite, the metabolite identity should be regarded as putative rather than exact for these metabolites.

Table 1 Metabolites identified by GC/MS as components of *Agaricus bisporus*

<i>Fatty Acids</i>	<i>Phenolics</i>	<i>Amino Acids</i>	<i>Sugars & Polyols</i>	<i>Organic Acids</i>	<i>Others</i>
Dodecanoic acid	Benzoic acid [°]	Alanine [°]	D-mannose	Acetic acid*	Pyrimidine
Tridecanoic acid	2-(4-methoxyphenyl)ethanol	Asparagine	D-fructose ^{*°}	Gluconic acid	Urea*
Tetradecanoic acid	Diphenyl ether [°]	Glycine	D-ribose*	Saccharic acid	Benzene
Pentadecanoic acid	2,6-bis(1,1-dimethylethyl)-4-chloro-phenol	Aspartic acid	Erythrose*	Succinic*	Silanamine
Hexadecanoic acid [°]	8-phenyl-6-thio-theophylline	Proline [°]	α-D-glucopyranoside-α-D-fructofuranosyl	Citric acid [°]	3-octanol*
trans-9-Hexadecenoic acid	Tyrosine [°]	Threonine	D-glucitol	Phthalic acid	
Heptadecanoic acid [°]	3,4-dihydrobenzyl alcohol	Tryptophan	D-ribo-hexitol	Propanedioic acid	
Octadecanoic acid [°]	1,3,8-trihydroxy-6-methylanthraquinone*	Valine [°]	Inositol [°]	Quinaldic acid*	
9,12-Octadecadienoic acid [°]	phenol 2,4-bis(1,1-dimethylethyl)*	Serine [°]	Glycerol [°]	3-acetoxy-3-hydroxypropionic acid	
Eicosanoic acid [°]	4-phenyl-2-hydroxystilbene*	Glutamine*		Pentanedioic acid*	
Heneicosanoic acid*					
Tricosanoic acid*					
11-Eicosanoic acid*					
9,15-Octadecadienoic acid*					
Ricinoleic acid*					
Erucic acid*					
Docosanoic acid*					
Hexanoic acid *					

* Metabolites found in a low percentage of sample (>10% & less than 15%)

[°] Metabolites verified by authentic reference compound

Compounds identified with very high probabilities (similarity coefficient or reverse similarity coefficient >85%) are indicated in bold

3.2. Detection of Damage

3.2.1. Principal Component Analysis (PCA)

Samples were studied separately on the basis of their tissue type, that is caps, gills and stipes and also on their age i.e. day zero and day one. The score plot for day zero caps is shown in Figure 1a for PC1 vs PC2; these first two principal components accounted for 50 and 40% respectively of the total variance in the GC/MS data set. Separation between some samples on the basis of damage is readily apparent. The majority of UD caps formed a cluster on the score plot. D20 samples also showed evidence of clustering on the score plot. D40 samples were spread randomly throughout the score plot.

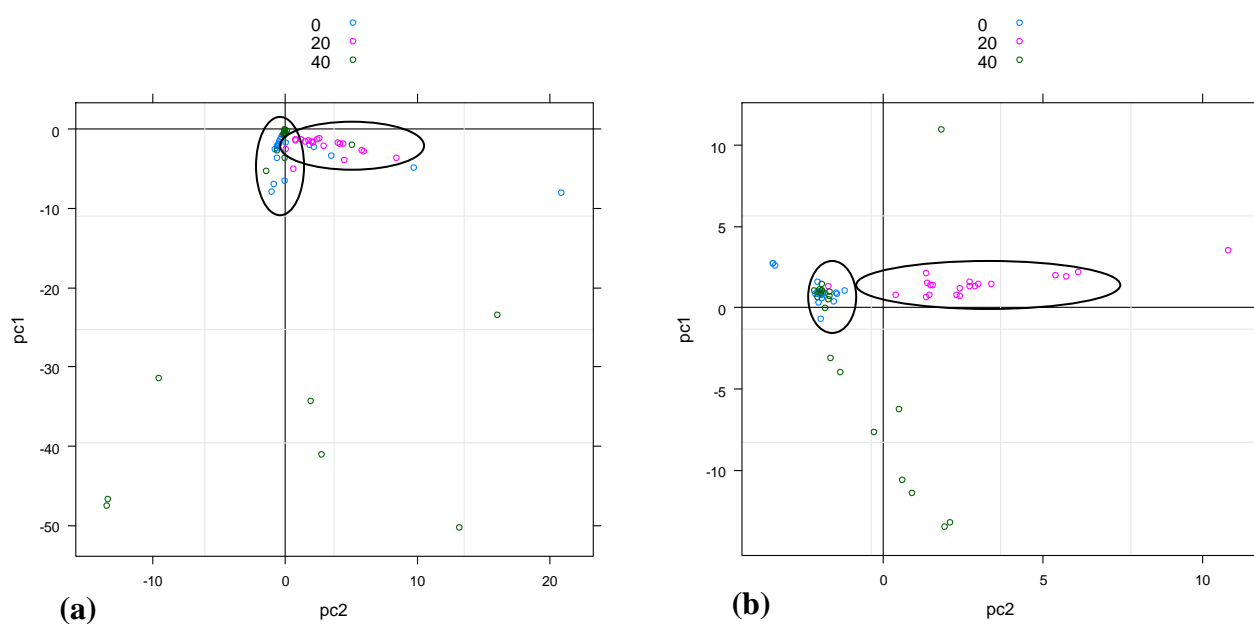


Figure 1 PC1 vs PC2 score plots for cap tissue for (a) Day zero samples and (b) Day one samples
0: undamaged, 20: 20 min damage, 40: 40 min damage

In the case of day one caps (Figure 1b) a pattern can again be seen in the score plot for PC1 vs PC2 (accounting for 64 and 25% of the total variance), clusters were seen for UD and D20 samples indicating that metabolite levels are affected by damage.

In the case of gill and stipe tissue, clusters for different damage levels were not clearly evident, with overlapping of damage levels seen for both day zero and day one.

3.2.2. *Random Forests (RF)*

A total of 7 RF models were built using the GC/MS data. The first model developed attempted to discriminate damaged from undamaged samples (using all of the data) and to identify specific metabolites that could be used as possible markers for damage in mushrooms. The model tried to predict damage in mushrooms using all the metabolites identified by GC/MS, a variable indicating the tissue from which the metabolite originated (cap, gill or stipe), and the age of the sample as explanatory variables. This resulted with a model with good classification with an out-of-bag (OOB) error rate of 11.11%, sensitivity 88.9% and specificity 92%. The variable of importance (VIP) plot for predicting damage indicated pentadecanoic acid, linoleic acid, myo-inositol, benzoic acid and hexadecanoic acid as the five most important metabolites that could be used as markers for damage (Figure 2).

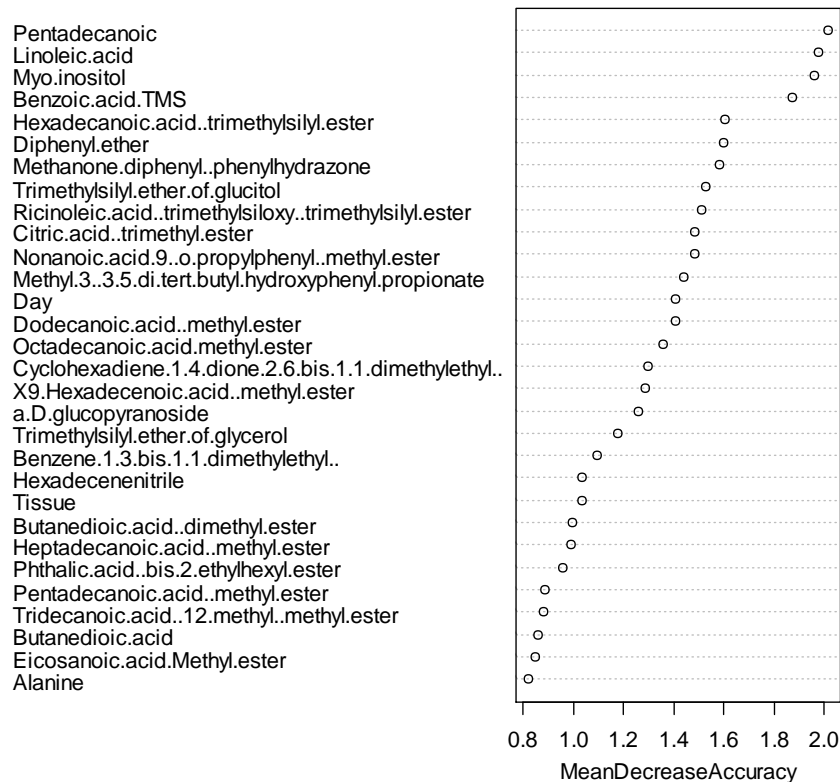


Figure 2 VIP plot of metabolites that are important variables in the RF model for predicting damage

By removing the variable age and tissue from the model a second model was built (all data used). This RF could be used as a classifier of mushroom damage and gave a good prediction with an OOB error rate of 11.39%, sensitivity 88.6% and specificity 92%. This meant that even receiving mushrooms whose age postharvest was unknown the model still performed well. The top five important variables for predicting damage in mushrooms were the same as the previous model (Figure 2).

Three RF models were then produced using data from each tissue type separately to discriminate damage in mushrooms. All models produced low error rates (>10%); with cap tissue having the lowest OOB error of just 8.33%, indicating that cap tissue alone could be used to predict damage. The important metabolites as indicated by the model were; linoleic acid, hexadecanoic acid, heptadecanoic acid, D-mannose and glycerol. A further two models were then built for each mushroom age (i.e. day zero

and day one samples). The model using day zero data produced an OOB error rate of 10%, whilst the RF model using day one samples resulted with an OOB of just 6.67%. It has been previously reported that the metabolic response in the form of enzyme expression in mushrooms to both age (Mohapatra *et al.*, 2008) and damage (O'Gorman *et al.*, 2010) is delayed in time and that it takes at least one day to develop. Therefore metabolite identification with day one samples is more significant when examining indicators of damage/aged metabolism; whereas the analysis of day zero samples will be useful to find early indicators of damage (before it is perceived by the consumer).

VIP plots were produced for each RF model. It was observed that fatty acids were the most important metabolite group for predicting damage in mushrooms (Table 2), with linoleic acid, pentadecanoic acid and hexadecanoic acid identified as important markers of damage by a number of models.

Univariate analysis (ANOVA) confirmed that the difference in concentrations of these metabolites was significant between damaged and undamaged samples and therefore could be used as markers for indicating damage in mushrooms.

Table 2 Summary of all RF models produced for predicting damage in mushrooms

<i>RF Model</i>	<i>OOB error rate</i> (%)	<i>Sensitivity & Specificity (%)</i>	<i>Important Metabolites</i>
Model 1 & 2 (all data used)	11.11 (1)	88.9 (1)	Pentadecanoic acid
	11.39 (2)	92.0 (1)	Linoleic acid
		88.6 (2)	Myo-inositol
		92.0 (2)	Benzoic acid
Model 3 (Caps)	8.33		Hexadecanoic acid
		95.0	Linoleic acid
		97.3	Hexadecanoic acid
			Heptadecanoic acid
			D-mannose
Model 4 (Gills)	13.3		Glycerol
		82.7	Myo-inositol
		90.0	Glucitol
			Citric acid
			Benzoic acid
Model 5 (Stipes)	9.17		D-ribo-hexitol
		92.0	Benzoic acid
		97.0	Propanedioic acid
			Serine
			D-ribo-hexitol
Model 6 (day zero)	10.0		Ricinoleic acid
		89.6	Linoleic acid
		92.0	Nonanoic acid
			Diphenyl ether
			Hexadecanoic acid
Model 7 (day one)	6.67		Pentadecanoic acid
		96.0	Phthalic acid
		98.5	Myo-inositol
			Pentadecanoic acid
			Glucitol
	Linoleic acid		

OOB: Out-of-bag error rate

3.2.3. Partial Least Squares-Discriminant Analysis (PLS-DA)

A PLS-DA model was developed to discriminate between the three levels of damage using all of the data i.e. all tissue types and mushroom ages. Accuracy was used to select the optimal model i.e. appropriate number of latent variables to be used in the model (Kuhn, 2008), the number used was 4 (Figure 3).

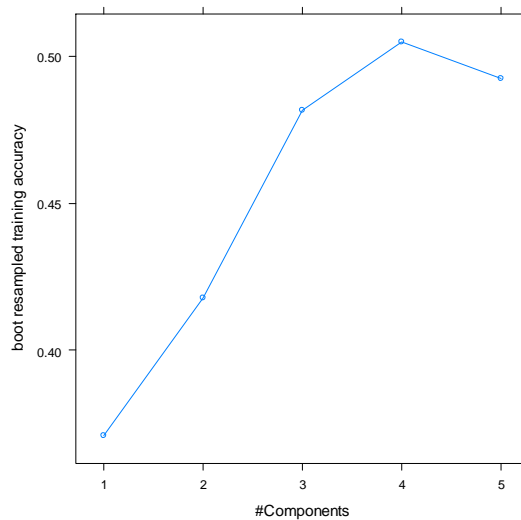


**Figure 3 Evolution of bootstrap resampling accuracy as a function of latent variables
#Components: Latent variable number/PLS loadings**

The initial PLS model was built using all of the data to evaluate whether it could differentiate between damaged and undamaged samples with high sensitivity and specificity. The results are presented in Table 3 containing the values of sensitivity (i.e. percentage of samples correctly classified as such) and specificity (i.e. percentage of samples from the other classes that are well classified by the model). The model did not perform well with an overall accuracy of just 55%. The training set performed with an overall accuracy of 53% and the test set an accuracy of 63%.

Table 3 Summary of results for mushroom discrimination on the basis of damage (all data)

<i>Damage Level (Minutes)</i>	<i>Sensitivity</i>	<i>Specificity</i>
0	86 ^a	46 ^a
	93 ^b	53 ^b
20	44 ^a	89 ^a
	48 ^b	96 ^b
40	29 ^a	93 ^a
	48 ^b	95 ^b

^a Training set, ^b Testing set

PLS-DA models were then developed to differentiate between damage levels for each tissue type. The models had the ability to detect undamaged samples quite well particularly for cap tissue, with high sensitivity and specificity (Table 4). The RF model produced using cap tissue also performed well for the discrimination of damage (OOB 8.3%), highlighting the usefulness of this tissue alone for predicting damage in mushrooms using PLS-DA and RF models.

Table 4 Performance statistics of PLS-DA models built using GC/MS data

<i>Damage Level (Minutes)</i>	<i>#LV</i>	<i>Tissue</i>	<i>Sensitivity</i>	<i>Specificity</i>
0	4	Cap	92 ^a , 97 ^b	76 ^a , 81 ^b
		Gills	74 ^a , 69 ^b	78 ^a , 60 ^b
		Stipes	76 ^a , 81 ^b	85 ^a , 82 ^b
20	4	Cap	69 ^a , 71 ^b	66 ^a , 72 ^b
		Gills	56 ^a , 61 ^b	79 ^a , 74 ^b
		Stipes	62 ^a , 54 ^b	71 ^a , 67 ^b
40	3	Cap	65 ^a , 75 ^b	80 ^a , 85 ^b
		Gills	36 ^a , 54 ^b	89 ^a , 81 ^b
		Stipes	45 ^a , 51 ^b	75 ^a , 80 ^b

^a Training set, ^b Testing set

#LV: Number of latent variables

Misclassification of samples was seen between D20 and D40 for all tissue types, however lower error rates were seen for cap tissue (training and testing models). Although the models did not perform well for differentiating between the damage levels (D20/D40) they did perform well for discriminating undamaged samples from

damaged ones, making PLS-DA an important tool for detecting damage in mushrooms.

Modeling damage in mushrooms has been reported in literature in recent times (Gowen *et al.*, 2008a; Gowen *et al.*, 2008b; Esquerre *et al.*, 2009; O'Gorman *et al.*, 2010; Taghizadeh *et al.*, 2010) using different techniques including fourier transform infrared spectroscopy, hyperspectral imaging and near infrared spectroscopy coupled with chemometrics. These studies yielded models with low error rates for predicting damage in mushrooms highlighting the usefulness of imaging and spectroscopy for detecting physical damage in mushrooms, with the possibility of using these tools to develop classification systems for the industry.

The use of GC/MS and chemometrics also produced models with low error rates for detecting damage. RF models indicated the important variables for discriminating damage i.e. specific metabolites that could be used as metabolic markers of damage in mushrooms. The ability to detect specific metabolites for damage allows the ability to gain understanding into metabolic pathways associated with the metabolites identified. Metabolomics (GC/MS) coupled with chemometrics has not to the authors knowledge been used to detect damage in mushrooms; however, it has been used as a tool in the food industry for similar use for e.g. identification of volatile quality markers for ready to use cabbage and lettuce (Lonchamp *et al.*, 2009). Metabolic profiling using GC/MS to profile metabolic changes in sound and brown pears was investigated using a PLS-DA multivariate statistical approach (Pedreschi *et al.*, 2009). GC/MS profiling has also found a function in determining phytochemical diversity in tubers of potatoes (Dobson *et al.*, 2008).

These examples highlight the usefulness of GC/MS profiling and when coupled with chemometrics have the ability to develop models to predict damage with low error rates, making it an invaluable tool for the mushroom industry.

3.3. Correlation of Metabolite Levels

Polar and non-polar metabolite groups were examined separately. Polar metabolites included the amino acids, sugars and polyols, whilst the non-polar metabolites were the fatty acids and phenolic compounds. Correlation between metabolites was examined for each damage level, tissue type and age respectively. There were 132 highly positively correlated pairs for day zero samples and 121 medium correlated metabolites. Of the highly correlated metabolites 93 were between fatty acids, 21 between amino acids, 13 between sugars and 5 between phenolic compounds. Day one samples resulted with 39 highly and 74 medium correlated metabolites. Of the highly correlated pairs 13 were between fatty acids, 13 between amino acids, 11 between phenolics and two between sugars.

3.3.1. Correlation Matrices (Non-polar Metabolites)

The highest numbers of highly correlated metabolites were found for cap tissue D40 samples (Figure 4). There were high correlations seen between saturated fatty acids with expected correlations between fatty acids with even carbon numbers (e.g. octadecanoic acid and eicosanoic acid) and between those with odd carbon numbers (e.g. pentadecanoic acid and heptadecanoic acid), the member of each series being biosynthetically sequentially from the same starting unit by the addition of a C₂ unit from malonyl-CoA (O'Hara *et al.*, 2002).

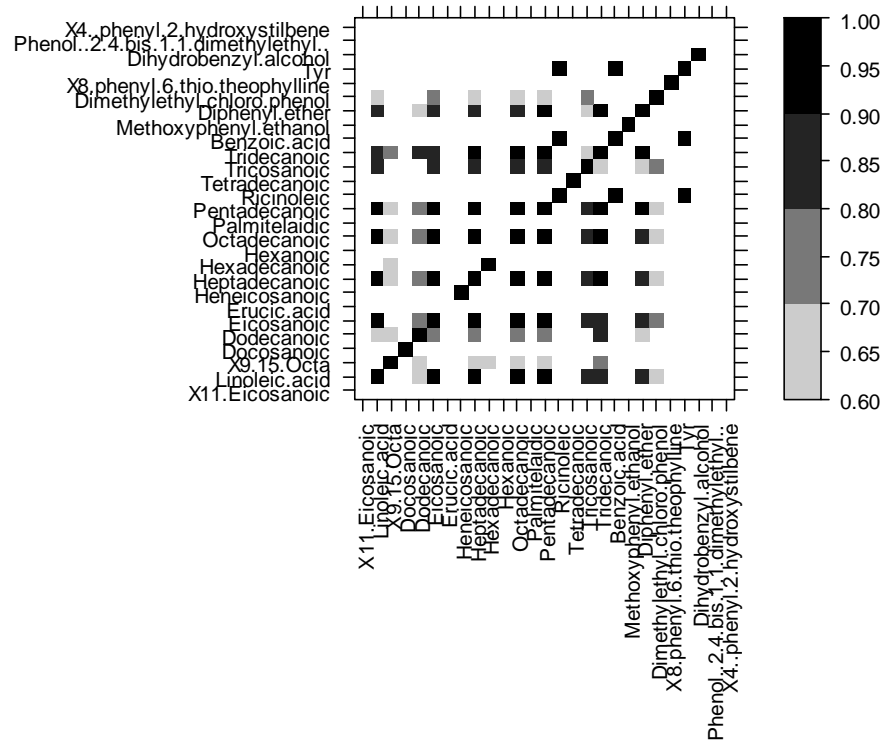


Figure 4 Correlation matrices of non-polar metabolites in day zero cap tissue after 40 min damage (D40)

Only a few correlations were seen between fatty acids and phenolic compounds in day zero cap samples, however, a number were found in day one samples that had been extensively damaged (D40). There were a total of 8 fatty acid and phenolic pair-wise correlations. Interestingly high correlations were seen between pentadecanoic acid and linoleic acid in day zero and day one (cap, gills and stipes) for samples that had been damaged (D20/D40). These two metabolites were not correlated in undamaged samples which suggests that a metabolic pathway (related to fatty acids and possibly membrane regeneration) becomes switched on when a mushroom becomes damaged. These two metabolites were also identified by a number of RF models as variables of importance for modeling damage in mushrooms. Figure 5 shows the response ratios

of linoleic acid and pentadecanoic acid for each tissue type at each day, highlighting the fact that the metabolites are not highly correlated in undamaged samples but are for damaged samples.

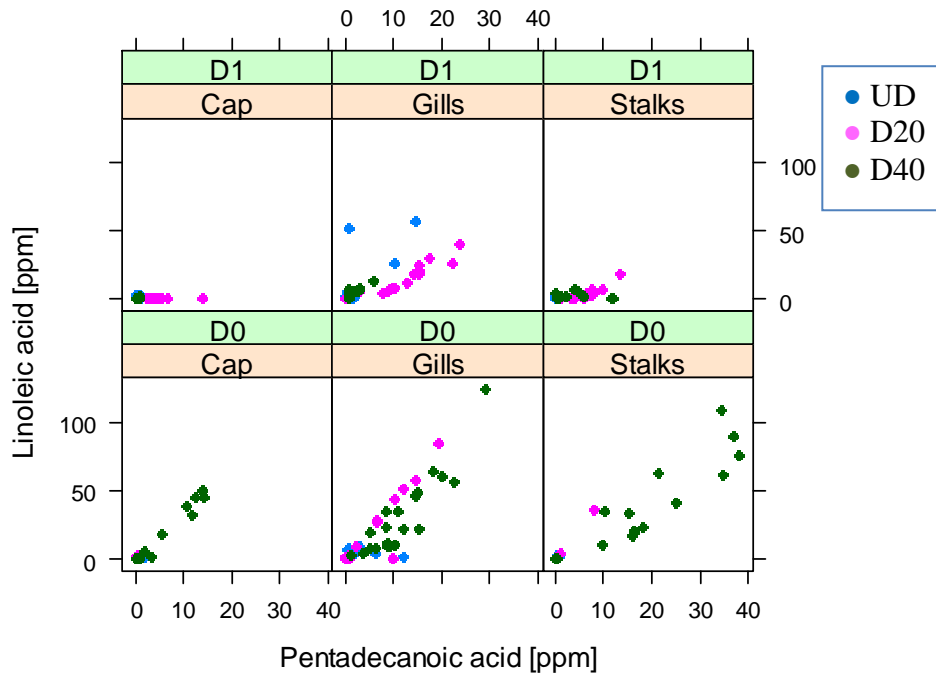


Figure 5 Plots of response ratios for linoleic and pentadecanoic acid for each tissue type and day.

3.3.2. Correlation Matrices (Polar Metabolites)

Figure 6 shows the correlation matrices for polar metabolites (day zero samples) for cap tissue. A striking feature of the data was the extent of correlation within amino acids in D20 samples (Figure 6b). There were a number of high correlations between amino acids and sugars/polyols such as glucitol and alanine, and myo-inositol and glycine (Figure 6a). Examples can also be seen in D40 samples; glycerol with alanine, glucitol with tyrosine and myo-inositol with proline etc (Figure 6c). Amino acids play important roles as basic substrates and as regulators in many metabolic pathways (Brosnan, 2003).

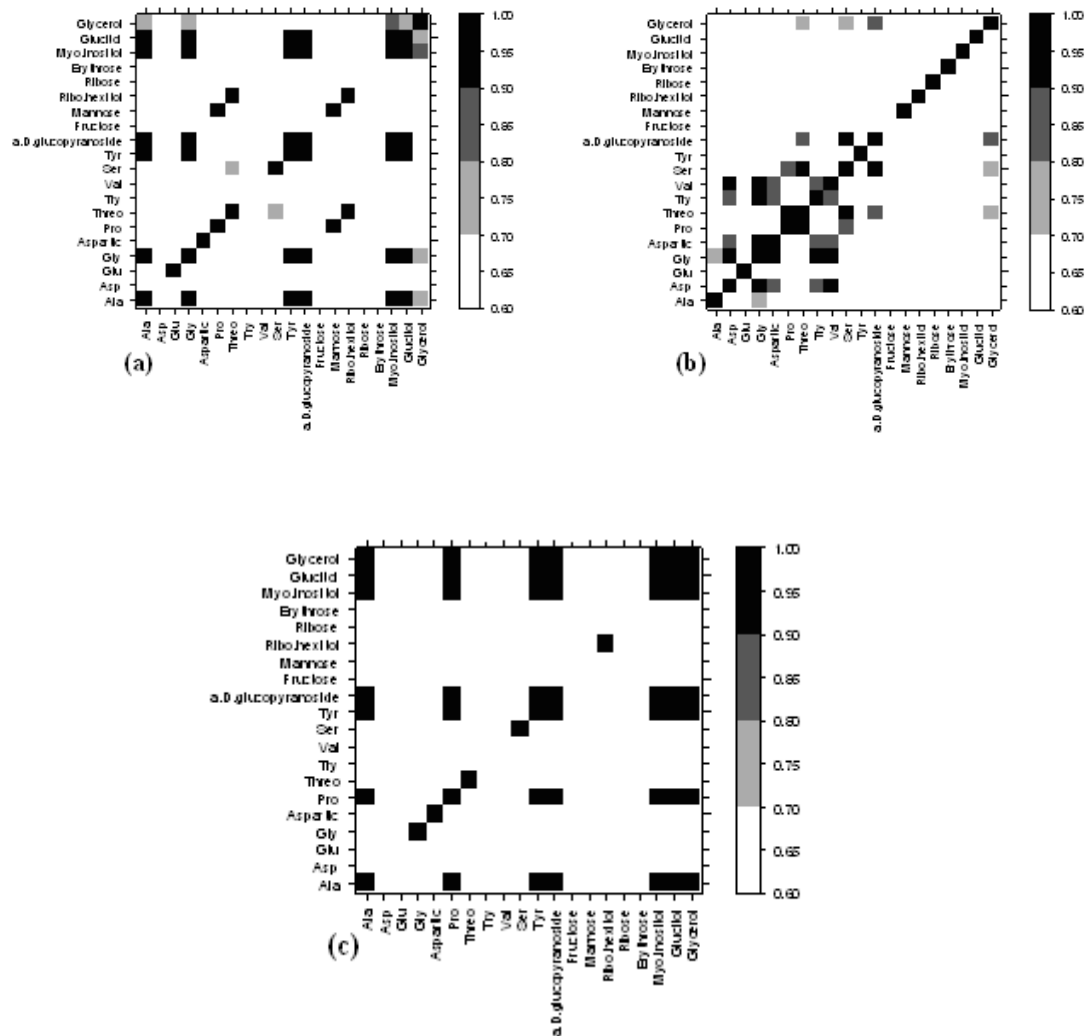


Figure 6 Correlation matrices of polar metabolites in day zero cap tissue (a) UD samples (b) D20 samples (c) D40 samples

Tyr: tyrosine, Ser: serine, Val: valine, Thy: threonine, Threo: threonine, Pro: Proline, Aspartic: aspartic acid, Gly: glycine, Glu: glutamine, Asp: asparagine, Ala: alanine

The correlation matrix for UD day zero cap samples (Figure 6a) showed a number of correlations between the same group of metabolites and also a number of inter-correlations for e.g. alanine with myo-inositol. The highly correlated metabolites between amino acids and sugars/polyols were not seen in D20 cap tissue; however a number of high correlations between amino acid metabolites were seen. The matrix for D40 samples had fewer correlations between amino acid metabolites, however an increase of inter-correlations were found, similar to the correlation matrix for UD

samples. Correlation matrices were also examined for gill and stipe tissue (day one samples). The same trends were observed for metabolites that were highly correlated. The observation of correlations shows that the metabolite concentrations are dependent on each other and therefore must be strongly connected to the underlying biophysical system. Cell metabolism constitutes a complex dynamical system, which is continuously subject to fluctuations. These fluctuations arise from a continuously environment and also from complex patterns of regulation, generated by the network itself. These fluctuations induce variability in certain metabolites, propagate through the network and generate an emergent pattern of correlations (Steuer *et al.*, 2003). The strong correlations between amino acids and sugars/polyols particularly in UD and D40 cap samples suggests the possibility that amino acid synthesis might be controlled, at least partly, by carbohydrates or associated factors.

Correlation matrices were also examined for day one samples. It was observed that a number of new correlations appeared in damaged samples (D20 and D40) which indicated the activation of new metabolic pathways through the effect of damage, affecting the ratios/relationships between the different metabolites and imply *de novo* enzyme production. Correlations of cap tissue (day one) show the adaption of mushroom metabolism to mechanical damage (Figure 7).

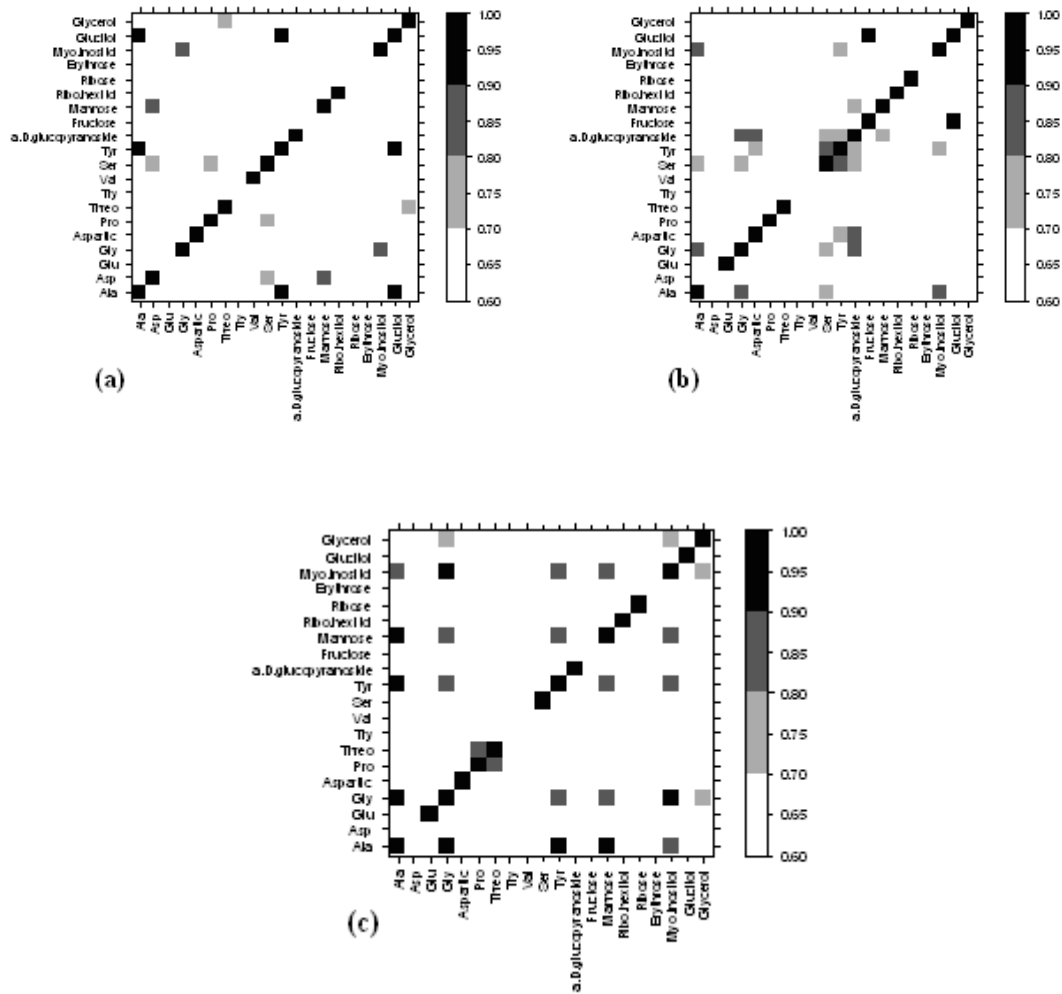


Figure 7 Correlation matrices of polar metabolites in day one cap tissues (a) 0 min damage (b) 20 min damage and (c) 40 min damage

Tyr: tyrosine, Ser: serine, Val: valine, Try: tryptophan, Threo: threonine, Pro: Proline, Aspartic: aspartic acid, Gly: glycine, Glu: glutamine, Asp: asparagine, Ala: alanine

Gill and stipe matrices were also examined with a number of correlations observed, however there was no trend seen that could be used to differentiate between damaged and undamaged mushrooms. However, correlation matrices are useful in understanding metabolic pathway interactions between metabolites. It seems that pathways controlling carbon and amino acid metabolism should cross-link, since amino acids are based on carbon skeletons (Morcuende *et al.*, 1998) and therefore correlations between these groups of metabolites were observed.

4. Concluding Remarks

The metabolic profiling tool GC/MS was employed in order to build a library of mushroom metabolites. Over 100 metabolites were separated and identified including carbohydrates, fatty acids, phenolic compounds, amino acids and polyols. Chemometric tools were successfully applied to GC/MS data to predict damage in mushrooms. RF models produced models with OOB errors of less than 10% and identified specific fatty acids as important markers of damage. PLS-DA models were also able to predict damage in mushrooms in an acceptable manner.

Correlation matrices were produced for non-polar and polar metabolites, with each tissue and age examined separately. A number of high correlations were found between each metabolite group and also inter-correlations between metabolites from different groups. Non-polar matrices indicated that linoleic acid and pentadecanoic acid were highly correlated within damaged samples but not in undamaged samples. These two metabolites were also identified by RF models as being important variables for predicting damage.

Hence, GC/MS coupled with chemometric methods have the ability to predict damage in mushrooms, with specific metabolites highlighted as possible markers of damage. Those markers could be used to further develop chemical sensors of early damage in production and export of mushrooms.

Acknowledgements

Thanks to Dr. Helen Grogan and Ted Cormican, Teagasc, Kinsealy Research Centre (Dublin, Ireland), for the supply of mushrooms and background information.

References

- Arbona, V., D.J. Iglesias, M. Talón and G.-C. A. (2009). Plant phenotype demarcation using nontargeted LC-MS and GC-MS metabolite profiling. Journal of Agricultural and Food Chemistry **57**(16): 7338-7347.
- Breiman, L. (2001). Random Forests. Machine Learning **45**: 5-32.
- Brosnan, T. and D.W. Sun (2004). Improving quality inspection of food products by computer vision--a review. Journal of Food Engineering **61**(1): 3-16.
- Burton, K.S. (2004). Cultural factors affecting mushroom quality - cause and control of bruising. Mushroom Science **16**: 397-402.
- Chang, S.T. and P.G. Miles, Eds. (2004). Mushrooms: Cultivation, Nutritional Value, Medicinal Effect and Environmental Impact, CRC Press.
- Dobson, G., T. Shepherd, S.R. Verrall, S. Conner, J.W. McNicol, G. Ramsay and D. Stewart (2008). Phytochemical diversity in tubers of potato cultivars and landraces using GC/MS metabolomics approach. Journal of Agricultural and Food Chemistry **56**: 10280-10291.
- Esquerre, C., A.A. Gowen, C. O'Donnell and G. Downey (2009). Initial studies on the quantitation of bruise damage and freshness in mushrooms using visible-near infrared spectroscopy. Journal of Agricultural and Food Chemistry **57**: 1903-1907.
- Fiehn, O. (2008). Extending the breadth of metabolite profiling by gas chromatography coupled to mass spectrometry. TrAC Trends in Analytical Chemistry **27**(3): 261-269.
- García-Cañas, V., C. Simó, C. León and A. Cifuentes (2010). Advances in Nutrigenomics research: Novel and future analytical approaches to investigate

- the biological activity of natural compounds and food functions. Journal of Pharmaceutical and Biomedical Analysis **51**(2): 290-304.
- Gibney, M.J., M. Walsh, L. Brennan, H.M. Roche, B. German and B. Ommen (2005). Metabolomics in human nutrition: opportunities and challenges. The American Journal of Clinical Nutrition **82**: 497-503.
- Gormley, T.R. and L. O'Sullivan (1975). Use of a simple reflectometer to test mushroom quality. The Mushroom Journal **34**: 344-346.
- Gowen, A.A., C.P. O' Donnell, M. Taghizadeh, P.J. Cullen, J.M. Frias and G. Downey (2008a). Hyperspectral imaging combined with principal component analysis for bruise damage detection on white mushrooms (*Agaricus bisporus*). Journal of Chemometrics **22**(3-4): 259-267.
- Gowen, A.A., C.P. O'Donnell, M. Taghizadeh, E. Gaston, A. O'Gorman, P.J. Cullen, J.M. Frias, C. Esquerre and G. Downey (2008b). Hyperspectral imaging for the investigation of quality deterioration in sliced mushrooms (*Agaricus bisporus*) during storage. Sensing and Instrumentation for Food Quality and Safety **2**(3): 133-143.
- Gowen, A.A., M. Taghizadeh and C.P. O'Donnell (2009). Identification of mushrooms subjected to freeze damage using hyperspectral imaging. Journal of Food Engineering **93**(1): 7-12.
- Jolivet, S., N. Arpin, H.J. Wichers and G. Pellon (1998). *Agaricus bisporus* browning: a review. Mycological Research **102**(12): 1459-1483.
- Kuhn, M. (2008). Building predictive models in R using the caret package. Journal of Statistical Software **28**(5): 1-26.

- Lisec, J., N. Schauer, J. Kopka, L. Willmitzer and A.R. Fernie (2006). Gas chromatography mass spectrometry-based metabolite profiling in plants. Nature Protocols **1**: 387-396.
- Lonchamp, L., C. Barry-Ryan and M. Devereux (2009). Identification of volatile quality markers of ready-to-use lettuce and cabbage. Food Research International **42**: 1077-1086.
- Moalemiyan, M., A. Vikram and A.C. Kushalappa (2007). Detection and discrimination of two fungal diseases of mango (cv. Keitt) fruits based on volatile metabolite profiles using GC/MS. Postharvest Biology and Technology **45**(1): 117-125.
- Mohapatra, D., J.M. Frias, F.A.R. Oliveira, Z.M. Bira and J. Kerry (2008). Development and validation of a model to predict enzymatic activity during storage of cultivated mushrooms (*Agaricus bisporus* spp.). Journal of Food Engineering **86**: 39-48.
- Morcuende, R., A. Krapp, V. Hurry and M. Stitt (1998). Sucrose-feeding leads to increased rates of nitrate assimilation, increased rates of alpha-oxoglutarate synthesis, and increased synthesis of a wide spectrum of amino acids in tobacco leaves. Planta **206**: 394-409.
- Needham, R., J. Williams, N. Beales, P. Voysey and N. Magan (2005). Early detection and differentiation of spoilage of bakery products. Sensors and Actuators B: Chemical **106**(1): 20-23.
- Norli, H.R., A. Christiansen and B. Holen (2010). Independent evaluation of a commercial deconvolution reporting software for gas chromatography mass spectrometry analysis of pesticide residues in fruits and vegetables. Journal of Chromatography A **1217**: 2056-2064.

- O'Gorman, A., G. Downey, A.A. Gowen, C. Barry-Ryan and J.M. Frias (2010). Use of fourier transform infrared spectroscopy and chemometric data analysis to evaluate damage and age in mushrooms (*Agaricus bisporus*) grown in Ireland. Journal of Agricultural and Food Chemistry **58**(13): 7770-7776.
- O'Hara, P., A.R. Slabas and T. Fawcett (2002). Fatty acid and lipid biosynthetic genes are expressed at constant molar ratios but different absolute levels during embryogenesis. Plant Physiology **129**: 310-320.
- Pedreschi, R., C. Franck, J. Lammertyn, A. Erban, J. Kopka, M.L.A.T.M. Hertog, B. Verlinden and B. Nicolai (2009). Metabolic profiling of 'Conference' pears under low oxygen stress. Postharvest Biology and Technology **51**: 123-130.
- R_Development_Core_Team (2009). R: a language and environment for statistical computing. V. R Foundation for Statistical Computing, Austria, 2007. UK.
- Roessner-Tunali, U., B. Hegemann, A. Lytovchenko, F. Carrari, C. Bruedigam, D. Granot and A.R. Fernie (2003). Metabolic profiling of transgenic tomato plants overexpressing hexokinase reveals that the influence of hexose phosphorylation diminishes during fruit development. Plant Physiology **133**(1): 84-99.
- Roessner, U., C. Wagner, J. Kopka, R.N. Trethewey and L. Willmitzer (2000). Simultaneous analysis of metabolite in potato tuber by gas chromatography-mass spectrometry. The Plant Journal **23**(1): 131-142.
- Schauer, N., D. Zamir and A.R. Fernie (2005). Metabolic profiling of leaves and fruit of wild species tomato: a survey of the *Solanum lycopersicum* complex. Journal of Experimental Botany **56**(410): 297-307.
- Steuer, R., J. Kurths, O. Fiehn and W. Weckwerth (2003). Observing and interpreting correlations in metabolomic networks. Bioinformatics **19**(8): 1019-1026.

- Taghizadeh, M., A. Gowen, P. Ward and C.P. O' Donnell (2010). Use of hyperspectral imaging for evaluation of the shelf-life of fresh white button mushrooms (*Agaricus bisporus*) stored in different packaging films. Innovative Food Science & Emerging Technologies **11**(3): 423-431.
- Teagasc (2007). The Irish agriculture and food development authority. Teagasc Mushroom Newsletter **29**.
- Vikram, A., B. Prithiviraj, H. Hamzehzarghani and A.C. Kushalappa (2004). Volatile metabolite profiling to discriminate diseases of McIntosh apple inoculated with fungal pathogens. Journal of the Science of Food and Agriculture **84**(11): 1333-1340.